Understanding the symmetry energy using data from the ALADIN-2000 Collaboration taken at the GSI Large Neutron Detector

Sanjeev Kumar and Y. G. Ma*
Shanghai Institute of Applied Physics, Chinese Academy of Sciences, Shanghai 201800, China
(Dated: November 26, 2012)

The present study deals with the extraction of the symmetry energy from heavy-ion collisions at intermediate energies. Using the isospin quantum molecular dynamical (IQMD) model, the dependence of the sum of the charge number for fragments with $Z \geq 2$ ($Z_{\rm bound}$) on the multiplicity of neutrons (M_n) from the projectile spectator fragmentation of ^{124}Sn and ^{124}La at 600 MeV/nucleon is compared with the experimental results of the ALADIN-2000 Collaboration. The comparison suggest a soft symmetry energy. In addition, the sensitivities of the symmetry energy towards the $Z_{\rm bound}$ dependence on proton multiplicity (M_p), neutron-to-proton single [$R(n/p)$] and double ratio [$R_D(n/p)$] are also examined. The $Z_{\rm bound}$ dependence of $R(n/p)$ is found to be the most sensitive observable towards the symmetry energy. The ALADIN Collaboration should extend the results for $R(n/p)$ in the near future.

PACS numbers: 21.65.Ef, 21.65.Cd, 25.70.Pq, 25.70.-z

There is an ongoing effort, within the nuclear physics and nuclear astrophysics communities, to constrain the density dependence of the symmetry energy (DDSE) [1–3]. Such constraints are also urgently needed because of the unique advantage of the DDSE in understanding the nuclear equation of state (NEOS) of asymmetric nuclear matter. In the last couple of years [2–13], heavy-ion collisions (HICs) at intermediate energies, due to their ability to cover the low-density as well as high-density region, have been considered an important tool for the determination of the sub- and supra-saturation density dependence of the symmetry energy. At present, the high-density behavior of the symmetry energy is of considerably greater uncertainty compared to the low-density behavior. However, a detailed analysis is still needed at low density in order to determine the specific characteristics such as the nucleon-nucleon cross section, the symmetry energy coefficient, method of clusterization etc. [4–6, 14]. Further progress in this direction will depend on the results from experiments that are still ongoing at laboratories worldwide.

At present, the results for the high-density behavior of the symmetry energy are interesting but vary drastically between models. In the following, we will give a brief overview of the theoretical as well as the combined theoretical and experimental progress. Theoretically, the single and double neutron-to-proton ratios [15, 16], single and double π^-/π^+ ratios [7–9, 15, 17], Σ^-/Σ^+ ratio [17], K^-/K^+ ratio [7], and isospin fractionation [16] are available as sensitive probes to study the high-density behavior of the symmetry energy. In addition, flow parameters are relevant. Flow in heavy-ion collisions is studied in terms of the relative and differential directed flow of neutron-to-proton, ^{3}H to ^{3}He [15], ratio and the difference [10, 11] of neutron-to-proton elliptic flow. Recently, the transverse emission of isospin ratios has also been suggested as a potential candidate for the determination of the symmetry energy [12].

In spite of considerable efforts, it is necessary to compare the theory with experimental findings. For example, in 2009, results from the FOPI collaboration for the π^-/π^+ ratio were compared with isospin-dependent Boltzmann-Uehling-Uhlenbeck (IBUU04) [8] and Lanzhou quantum molecular dynamics (LQMD) [9] model calculations. The results were in contradiction between the models. In 2011, neutron and proton elliptic flow at 400 MeV/nucleon was compared with findings from the FOPI Collaboration by two different groups [10, 11]. One group predicted the softness of the symmetry energy with $\gamma_i = 0.9$ using the ratio of neutron-to-proton elliptic flow [10]. The other group [11] also found evidence for a soft symmetry energy with $x = 2$ using the difference of neutron-to-proton elliptic flow. However, the approaches for the determination of the symmetry energy were different: in the first study, the symmetry energy was momentum independent, while in the latter one, it was obtained from momentum-dependent interactions. At the end of 2011 [13], the multiplicity of neutrons (M_n) data from projectile spectator fragmentation at 600 MeV/nucleon at GSI was compared with statistical multifragmentation model (SMM) calculations. The study pointed out the essential reduction in the strength of the symmetry energy. Even after the reduction of the symmetry energy coefficient, the data was reproduced satisfactorily only in the range $Z_{\rm bound}/Z_{\rm Projectile} \geq 0.5$.

It is clear that the statistical model failed to reproduce the data at low $Z_{\rm bound}$. This raises the important question whether a dynamical model provides an adequate description because the mechanism behind the statistical and dynamical models is different. In the present paper, we will try to answer this question by comparing the above experimental findings with isospin quantum molecular dynamical (IQMD) model [18] calculations. In the

*Author to whom all correspondence should be addressed: ygma@sinap.ac.cn

literature, no one has compared this data with dynamical model calculations in order to extract the symmetry energy. Success in this regard, to a certain extent, may help the community reduce the uncertainty in the determination of the symmetry energy. In addition, we will also check the sensitivity of the $Z_{\rm bound}$ dependence on the proton multiplicity(M_p), and the neutron-to-proton single [$R(n/p)$] and double ratios [$R_D(n/p)$] with regard to the symmetry energy. This will help in providing the most sensitive observable for the symmetry energy.

The study is performed within the framework of IQMD model. It has been applied successfully for the determination of isospin asymmetric nuclear matter equation of state. The isospin effects in the model have been included in terms of the symmetry potential, Coulomb potential, and isospin dependent nucleon-nucleon (NN) cross sections. In the model [18], nucleons are represented by the wave packets [19]. The time evolution of the nucleons, which are under the self-consistency generated mean field, is described by the well known Hamilton's equations of motion. The Hamilton (H) is the sum of the kinetic energy and effective interaction potential. The interaction potential is composed of Coulomb ($V_{\rm Coul}$), Yukawa ($V_{\rm Yukawa}$), local ($V_{\rm loc}$) and momentum dependent interactions ($V_{\rm MDI}$). The expressions for $V_{\rm Coul}$ and $V_{\rm Yukawa}$ have been derived by us and others in the Refs. [18]. The local interaction potential $V_{\rm loc}$ is originated from the Skyrme energy density function. On the basis of this, the local potential energy density is expanded as:

$$U_{\rm loc} = \frac{\alpha}{2}\frac{\rho^2}{\rho_0} + \frac{\beta}{\gamma+1}\frac{\rho^{\gamma+1}}{\rho_0^{\gamma}} + E_{\rm Sym}^{\rm pot}(\rho)\rho\delta^2, \quad (1)$$

where α, β, and γ are the parametrized values to specify the particular NEOS. The detailed table of the values is presented in the Ref. [18, 19].

The $E_{\rm Sym}^{\rm pot}$ is the symmetry potential energy, which is parametrized using the microscopic or phenomenological many body theory calculations. The total symmetry energy per nucleon employed in the simulation is the sum of the kinetic and potential terms and is given as

$$E_{\rm Sym}(\rho) = \frac{C_{\rm s,k}}{2}\left(\frac{\rho}{\rho_0}\right)^{2/3} + \frac{C_{\rm s,p}}{2}\left(\frac{\rho}{\rho_0}\right)^{\gamma_i}, \quad (2)$$

where $C_{\rm s,k} = \frac{\hbar^2}{3m}\left(\frac{3\pi^2\rho_0}{2}\right)^{2/3} \approx 25$ MeV is the symmetry kinetic energy coefficient and $C_{\rm s,p} = 35.19$ MeV is the symmetry potential energy coefficient.

The momentum dependent potential has been implemented from Ref.[19] and is expressed as following: $V_{\rm MDI} = C_{\rm mom}\ln^2[\epsilon(\Delta p)^2+1]\frac{\rho}{\rho_0}\delta(r'-r)$. Here $C_{\rm mom} = 1.57$ MeV and $\epsilon = 5\times10^{-4}\frac{c^2}{MeV^2}$. The momentum is given in units of MeV/c.

Finally, combining all the potentials, we got an isospin, density and momentum dependent single particle potential in nuclear matter, which is written as follow:

$$\begin{aligned} V_\tau(\rho,\delta,p) &= \alpha\left(\frac{\rho}{\rho_0}\right) + \beta\left(\frac{\rho}{\rho_0}\right)^{\gamma} + E_{\rm Sym}^{\rm pot}(\rho)\delta^2 \\ &+ \frac{\partial E_{\rm Sym}^{\rm pot}(\rho)}{\partial\rho}\rho\delta^2 + E_{\rm Sym}^{\rm pot}(\rho)\rho\frac{\partial\delta^2}{\partial\rho_{\tau,\tau'}} \\ &+ C_{\rm mom}\ln^2[\epsilon(\Delta p)^2+1]\frac{\rho}{\rho_0}. \end{aligned} \quad (3)$$

Here $\tau \neq \tau'$, $\frac{\partial\delta^2}{\partial\rho_n} = \frac{4\delta\rho_p}{\rho^2}$, and $\frac{\partial\delta^2}{\partial\rho_p} = \frac{-4\delta\rho_n}{\rho^2}$.

In the present simulations, the parameters α, β, and γ are -390 MeV, 320 MeV and 1.14, respectively. They give rise to the soft momentum dependent equation of state (SMD). The γ_i parameter in Eq. 2 describes the strength of the symmetry energy. The $\gamma_i = 0.5$ and 1.5 refe to the soft and hard symmetry energies, resepectively. Moreover, the isospin and energy dependent NN cross section in the collision term and the quantum feature in terms of Pauli blocking is implemented.

Following the experimental technique [13], the neutron and proton multiplicity is calculated using the cluster recognization method. In this method, the particles with relative momentum smaller than $P_{\rm Fermi}$ and relative distance smaller than R_0 are coalesced into one cluster. In the present work, the value of R_0 and $P_{\rm Fermi}$ are 3.5 fm and 268 MeV/c, respectively.

In order to perform the analysis, we have simulated thousands of event for the reactions of ^{124}Sn+^{nat}Sn and ^{124}La+^{nat}Sn at incident energy 600 MeV/nucleon along the whole Z_{bound} range. The effect of different targets on the projectile fragmentation is also observed by simulating the reaction of ^{124}Sn+^{124}Sn. In the figures, the horizontal (vertical) bar around the displayed symbols is the actual $Z_{\rm bound}$ bin size (error bar as 95% confidence level). The 95% confidence level is ± Standard Deviation (S.D.). The different colored lines with the same colored symbols are drawn spline to guide the trend of the different data points as well as reader's eyes.

It is important to realize the following experimental filters in the theoretical simulations: (1) the rapidity distribution cut for the projectile spectator fragmentation region, and (2) the correlation between the $Z_{\rm bound}$ and impact parameter (b) [20]. For the first factor, in Fig. 1(a), the $Z_{\rm bound}$ dependence of the rapidity distribution of neutrons for ^{124}Sn+^{nat}Sn at 600 MeV/nucleon is displayed. At low $Z_{\rm bound}$, a single Gaussian shape distribution is observed, which is found to split into two Gaussians at higher $Z_{\rm bound}$. From here and with the help of literature [21], the mid-rapidity region is specified around the zero value of rapidity. It is changing into projectile (target)-like matter towards the negative (positive) rapidity values. Using the experimental technique [13], the projectile spectator region in the theoretical calculations is found to be around -0.9 rapidity value. For the second factor, in Fig. 1(b), the impact parameter dependence of $Z_{\rm bound}$ is displayed. The $Z_{\rm bound}$ is calculated at different absolute impact parameters. The Z_{bound} increases linearly with the impact parameter. It illustrates that the

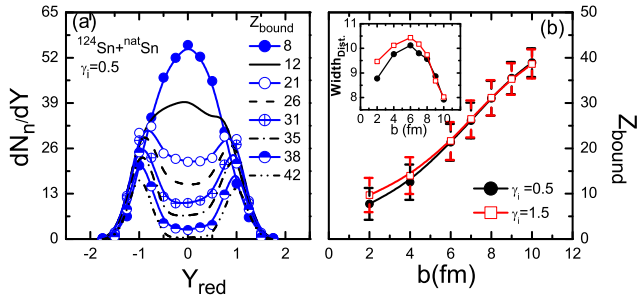

FIG. 1: (Color online) (a) Rapidity distribution of neutrons for ^{124}Sn+^{nat}Sn at 600 MeV/nucleon. The different lines and symbols correspond the values at different $Z_{\rm bound}$. (b) Impact parameter dependence of $Z_{\rm bound}$ with soft (solid circle with black line) and hard (open square with red line) symmetry energy. The inset is the impact parameter dependence of the width of $Z_{\rm bound}$ distribution.

correlation between the two parameters in the dynamical model agrees with the experimental viewpoint. After the above confirmation, in the rest of the analysis, the $Z_{\rm bound}$ is divided into different bins with the size ± 2.5 (Fig. 2-5) by considering the triangular distribution of the impact parameter.

In Fig. 1(b), the sensitivity of the symmetry energy on the impact parameter dependence of $Z_{\rm bound}$ is also checked. No sensitivity is observed at peripheral geometries, while the visible sensitivity has been found below semi-central geometries. This provides an indication of the larger $Z_{\rm bound}$ with the hard symmetry energy. It is possible because of different mechanism for $Z_{\rm bound}$ at central and peripheral geometries [22]. To assure that the visible sensitivity of the symmetry energy is whether or not due to the statistical error, the concept of width of $Z_{\rm bound}$ distribution is used. The width of distribution is full width at half maximal (FWHM), which is calculated as $2.35\times$ S.D.. The inset in the figure displays the impact parameter dependence of width of $Z_{\rm bound}$ distribution with the soft and hard symmetry energy. The symmetry energy sensitivity of width of $Z_{\rm bound}$ distribution resembles with the Z_{bound} distribution, indicating sensitivity of impact parameter selector (Z_{bound}) to the symmetry energy is due to the statistical fluctuations. This is understandable as $Z_{\rm bound}$ is a global variable, where the symmetry energy sensitivity becomes weak. In the following, we need to search for some potential sensitive observables.

In the left panels of Fig. 2, the $Z_{\rm bound}$ dependence of M_n from the projectile spectator decay is displayed. The first two panels in the figure are compared with the experimental data of the ALADIN-2000 Collaboration [13]. Identical to the experimental data, the neutron-rich projectile exhibits a maximum of neutrons $M_n \approx 11$ for ^{124}Sn and $M_n \approx 9$ for ^{124}La at the value of $Z_{\rm bound}/Z_{\rm Projectile} \approx 0.7$ in the presence of the soft symmetry energy. Above this $Z_{\rm bound}$, more neutrons are bound inside fragments and hence the multiplicity of neutrons decreases.

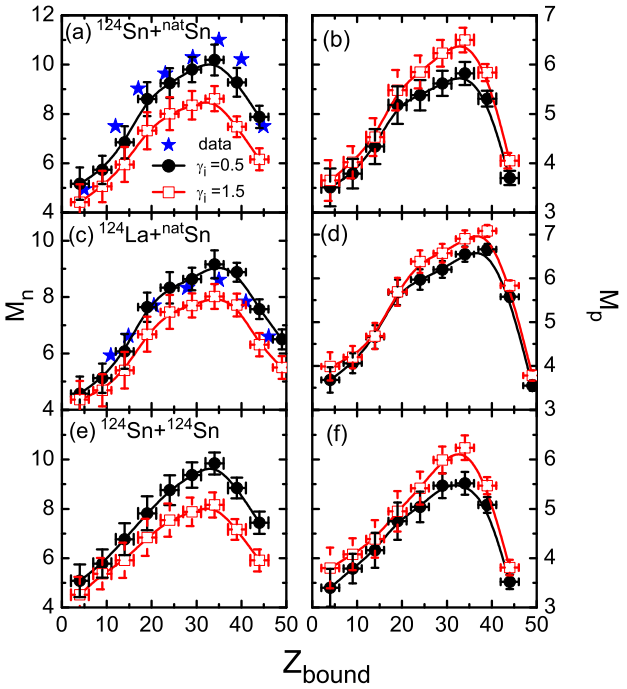

FIG. 2: (Color online) $Z_{\rm bound}$ dependence of M_n (M_p) in left (right) panels from projectile spectator fragmentation for different projectile-target combinations. The open square (solid circle) including lines have the same meaning as in the (b) part of the Fig. 1. The experimental data of ALADIN Collaborations is displayed by blue stars.

Interestingly, the multiplicity of neutrons presents sensitivity to the strength of the symmetry energy. In all the panels, the soft symmetry energy yields more neutrons compared to the hard symmetry energy. The sensitivity towards the symmetry energy has been seen more clearly from the more neutron-rich projectile ^{124}Sn compared to the neutron-poor ^{124}La. The previous comparison with the SMM calculations reproduced the data satisfactorily only in the range $Z_{\rm bound}/Z_{\rm Projectile} \geq 0.5$. The present IQMD model reproduces the experimental data along the whole $Z_{\rm bound}$ range. However, some discrepancies are observed for neutron-poor projectile ^{124}La compared to neutron-rich projectile ^{124}Sn. This depends on the different strength of the symmetry energy and Coulomb interactions in different projectiles. Owing to the more neutron-rich nature of ^{124}Sn, stronger symmetry energy effect has been observed and hence a good agreement with the data is obtained. While in case of ^{124}La, due to the presence of 4 extra protons compared to ^{124}Sn, the contribution from Coulomb interactions results in the deviation of the calculations from the experimental data. The enhanced production of protons in Fig. 2(d) compared to Fig. 2(b) is further supporting the discrepancies.

In addition, the multiplicity of neutrons from the projectile spectator fragmentation is strongly dependent on the type of projectile [(a) and (c)], while, is weakly dependent on the type of the target [(a) and (e)]. The related study has also been conducted at relatively low energy 25

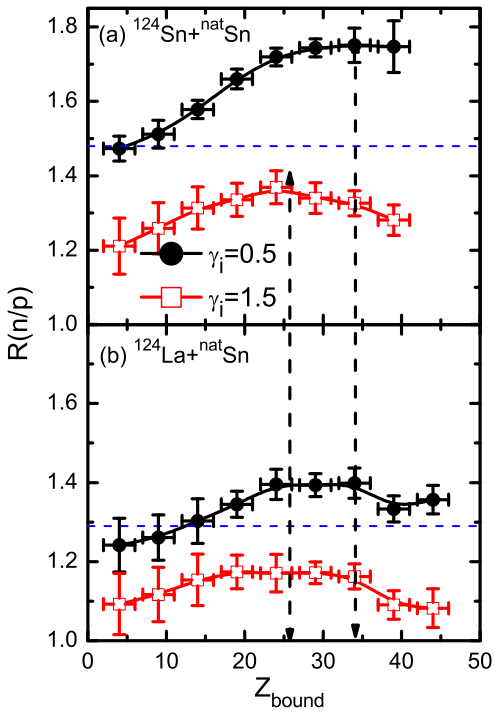

FIG. 3: (Color online) $Z_{\rm bound}$ dependence of $R(n/p)$ for neutron-rich (neutron-poor) ^{124}Sn (^{124}La) projectile spectator fragmentation in top (bottom) panels. The symbol and lines have the same meaning as in Fig. 2. The vertical dashed lines correspond to rough peak positions of $Z_{\rm bound}$ for $R(n/p)$ with hard and soft symmetry energy, respectively (from left to right).

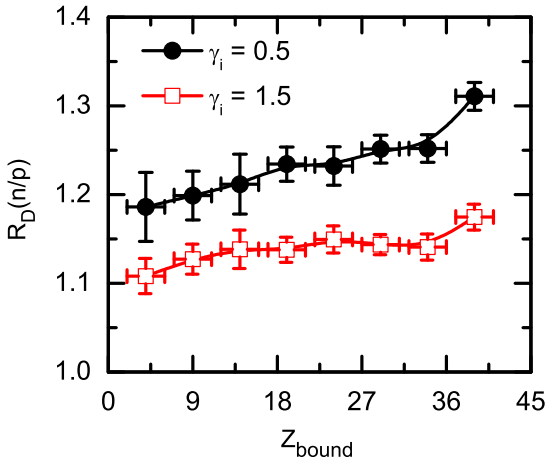

FIG. 4: (Color online) $Z_{\rm bound}$ dependence of double neutrons to protons ratio ($R_D(n/p) = \frac{R(n/p)\ for\ ^{124}Sn}{R(n/p)\ for\ ^{124}La}$) with soft and hard symmetry energy.

MeV/nucleon for ^{40}Ca + ^{40,48}Ca, ^{46}Ti reactions at the 4π CHIMERA detector [23]. They showed that competition between fusion-like and binary reactions in selected centrality bin can constrain the parametrization of the symmetry energy.

In the right panels of Fig. 2, the $Z_{\rm bound}$ dependence of proton multiplicity M_p from the projectile spectator decay is displayed. The behavior of the curves resembles with the left panels. The differences between the left and right panels are as follows: (1) The M_p is more with the hard symmetry energy, which was true with the soft for the M_n. This is because of the repulsive (attractive) nature of symmetry energy for neutrons (protons). At the freeze-out time, the soft symmetry energy has high magnitude, which will lead to the production of neutrons. It has alternatively led to the less production of protons; (2) More protons are produced for neutron-poor projectile ^{124}La compared to the neutron-rich projectile ^{124}Sn; (3) The sensitivity of symmetry energy is weak on the M_p in ^{124}La projectile, which is due to the dominance of Coulomb interactions. These factors are revealing the importance of the symmetry energy for neutron-rich reactions.

Now we will analyze the $Z_{\rm bound}$ dependence of neutron-to-proton single ratio $R(n/p)$ from the projectile spectator decay. In Fig. 3, the $R(n/p)$ is displayed for the ^{124}Sn+^{nat}Sn (top panel) and ^{124}La+^{nat}Sn (bottom panel) reactions. The single ratio is found to be more sensitive towards the soft symmetry energy. Particularly, the $R(n/p)$ with the soft (hard) symmetry energy is higher (lower) than the ratio of system [shown by blue horizontal line]. This is attributable to the large (small) magnitude of soft (hard) symmetry energy at freeze-out time. In addition, Figs. 2 and 3 has some similarities and differences. The behavior of the single ratio curves almost resemble with the $Z_{\rm bound}$ dependence of M_n and M_p, i.e. it also exhibits a maximum or saturates with $Z_{\rm bound}$. The difference is that the maximal value for $R(n/p)$ is noticed at different $Z_{\rm bound}/Z_{\rm projectile}$ with the soft (at 0.7) and hard (at 0.5) symmetry energy, which was at the same $Z_{\rm bound}/Z_{projectile}$ for the maximal M_n and M_p (at ≈ 0.7). It means that the single ratio has more (less) neutron-rich effects along $Z_{\rm bound}$ with the soft (hard) symmetry energy. This is once again due to different strength of symmetry energy and Coulomb interactions originated from the soft and stiff parametrization of the symmetry energy.

As discussed in the Ref. [4], the double neutron-to-proton ratio $R_D(n/p)$ from the two isotopes of a system is the most sensitive observable for the determination of the symmetry energy. In the present study, the projectiles are isobars and not the isotopes. The $Z_{\rm bound}$ dependence of $R_D(n/p)$ using the isobars is shown in Fig. 4. From the comparison of Fig. 3 with Fig. 4, it is found that the $Z_{\rm bound}$ dependence of the single as well as double ratio is more sensitive to the soft symmetry energy. In contrary, the double ratio, comparing to the single ratio, has relatively weak sensitivity toward the symmetry energy along the whole $Z_{\rm bound}$ region. Moreover, the $R_D(n/p)$ with the hard symmetry energy is weakly dependent on the $Z_{\rm bound}$. This may be the effect of four extra protons in the ^{124}La projectile, where the contribution from the Coulomb interactions can not be canceled,

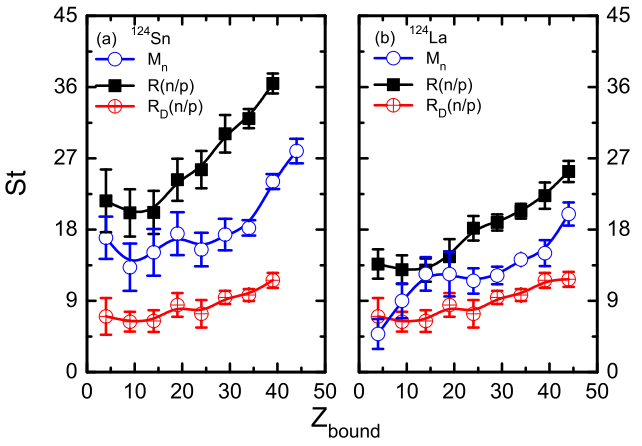

FIG. 5: (Color online) Z_{bound} dependence of sensitivity of different observables (shown in Fig. 2, 3, and 4) towards the symmetry energy. (a) for ^{124}Sn+^{nat}Sn and (b) for ^{124}La+^{nat}Sn.

even by taking the double ratio.

Finally, to declare the most sensitive observable toward the symmetry energy among the all three, i.e. M_n, $R(n/p)$, and $R_D(n/p)$, we have defined the sensitivity factor (St) as follow

$$St = \frac{|X_{\gamma_i=0.5} - X_{\gamma_i=1.5}|}{X_{\gamma_i=1.5}} \times 100 \qquad (4)$$

where $X = M_n$, $R(n/p)$ or $R_D(n/p)$.

From the results of St (Fig. 5), we can see that the St values for all the parameters are more sensitive for neutron-rich projectile, illustrating that neutron-rich nucleus is a good candidate for the extraction of the symmetry energy. As was expected from Fig. 4, the St factor of $R_D(n/p)$ shows the least sensitivity to the symmetry energy in this particular situation of different isobars. Between the other two, i.e. M_n and $R(n/p)$, the $R(n/p)$ shows more sensitivity to the symmetry energy. This sensitivity becomes more stronger with the increase of $Z_{\rm bound}$. Therefore, it is advisable that experimental Collaboration should also make the data for the $R(n/p)$ available, which can help to check the validity of our results for $R(n/p)$ and $R_D(n/p)$.

In conclusion, using the IQMD model, the ALADIN-2000 Collaboration data for multiplicity of neutrons extracted from the projectile spectator fragmentation is satisfactorily reproduced with the soft symmetry energy. Along with multiplicity of neutrons, proton multiplicity has also a peak around $Z_{\rm bound}/Z_{\rm porjectile} \approx 0.7$ with the soft as well as the hard symmetry energy. Interestingly, the $R(n/p)$ produced a peak around $Z_{\rm bound}/Z_{\rm porjectile} \approx 0.7$ (0.5) with the soft (hard) symmetry energy. The $R(n/p)$ for the different isobar projectiles is the most sensitive observable towards the symmetry energy in comparison to multiplicity as well as $R_D(n/p)$. In the near future, we hope experimental Collaborations make the results for proton multiplicity and $R(n/p)$ available.

This work is supported in part by the Major State Basic Research Development Program of China under Contract No. 2013CB834405, the Chinese Academy of Sciences Program for young international scientists under the Grant No. 2010Y2JB02, the NSFC of China under contract No. 11035009 and No, 10979074, and the Knowledge Innovation Project of the Chinese Academy of Sciences under Grant No. KJCX2-EW-N01.

[1] J. M. Lattimer and M. Prakash, Science **304**, 536 (2004); D. T. Loan *et al.*, Phys. Rev C **83**, 065809 (2011).
[2] B. A. Li, L.W. Chen, and C. M. Ko, Phys. Rep. **464**, 113 (2008).
[3] J. B. Natowitz *et al.*, Phys. Rev. Lett. **104**, 202501 (2010); L. Qin *et al.*, Phys. Rev. Lett. **108**, 172701 (2012).
[4] M. B. Tsang *et al.* , Phys. Rev. Lett. **102**, 122701 (2009); D.D.S. Coupland *et al.,* Phys. Rev. C **84**, 054603 (2011).
[5] Z. Y. Sun *et al.*, Phys. Rev. C **82**, 051603 (R) (2010).
[6] S. Kumar, Y. G. Ma, G. Q. Zhang, and C. L. Zhou, Phys. Rev. C **84**, 044620 (2011); *ibid.* **85**, 024620 (2012).
[7] H. H. Wolter *et al.* , Prog. Part. Nucl. Phys. **62**, 402 (2009).
[8] Z. G. Xiao, B. A. Li, L. W. Chen, G. C. Yong, and M. Zhang, Phys. Rev. Lett. **102**, 062502 (2009).
[9] Z. Q. Feng and G. M. Jin, Phys. Lett. B **683**, 140 (2010).
[10] P. Russotto *et al.*, Phys. Lett. B **697**, 471 (2011).
[11] M. D. Cozma, Phys. Lett. B **700**, 139 (2011).
[12] Z. Q. Feng, Phys. Lett. B **707**, 83 (2012).
[13] W. Trautmann *et al.*, PoS BORMIO **2011**, 018 (2011), arXiv:1108.5528v1.
[14] B. A. Li, C.M. Ko, and Z.Z. Ren, Phys. Rev. Lett. **78**, 1644 (1997); M. B. Tsang *et al.*, Phys. Rev. Lett. **92**, 062701 (2004); M. A. Famiano *et al.*, Phys. Rev. Lett. **97**, 052701 (2006).
[15] B. A. Li, Phys. Rev. Lett. **88**, 192701 (2002); S. Gautam *et al.,* Phys. Rev. C **83**, 034606 (2011); *ibid* **82**, 014604.
[16] B. A. Li, L. W. Chen, H. R. Ma, J. Xu, and G. C. Yong, Phys. Rev. C **76**, 051601 (R) (2007).
[17] Q. Li, Z. Li, E. Zhao, and R. K. Gupta, Phys. Rev. C **71**, 054907 (2005).
[18] C. Hartnack *et al.*, Eur. Phys. J. A **1**, 151 (1998).
[19] J. Aichelin, Phys. Rep. **202**, 233 (1991); E. Lehmann *et al.*, Prog. Part. Nucl. Phys. **30** , 219 (1993); R. K. Puri and J. Aichelin, J. Comput. Phys. **162** , 245 (2000).
[20] A. Schuttauf *et al.,* Nucl. Phys. A **607**, 457 (1996).
[21] S. Kumar, S. Kumar, and R. K. Puri, Phys. Rev .C **81**, 014601 (2010); S. Gautam, A. D. Sood, R. K. Puri, and J. Aichelin, Phys. Rev. C **83**, 014603 (2011).
[22] Y. K. Vermani and R. K. Puri, Europhys. Lett. **85**, 62001 (2009); S. Gautam *et al.,* Phys. Rev. C **85**, 067601 (2012).
[23] F. Amorini *et al.,* Phys. Rev. Lett. **102**, 112701 (2009).